GABAergic Actions Mediate Opposite Ethanol Effects on Dopaminergic Neurons in the Anterior and Posterior Ventral Tegmental Area

Yanzhong Guan, Cheng Xiao, Kresimir Krnjević, Guiqin Xie, Wanhong Zuo, and Jiang-Hong Ye

Department of Anesthesiology, Pharmacology, and Physiology, University of Medicine and Dentistry of New Jersey, New Jersey Medical School, Newark, New Jersey (Y.G., C.X., G.X., W.Z., J.-H.Y.); and Department of Physiology, McGill University, Montréal, Canada (K.K.)

ABSTRACT

It is known that the posterior ventral tegmental area (p-VTA) differs from the anterior VTA (a-VTA) in that rats learn to self-administer ethanol into the p-VTA, but not into the a-VTA. Because activation of VTA dopaminergic neurons by ethanol is a cellular mechanism underlying the reinforcement of ethanol consumption, we hypothesized that ethanol may exert different effects on dopaminergic neurons in the p-VTA and a-VTA. In patch-clamp recordings in midbrain slices from young rats (postnatal days 22-32), we detected no significant difference in electrophysiological properties between p-VTA and a-VTA dopaminergic neurons. However, acute exposure to ethanol (21–86 mM) stimulated p-VTA dopaminergic neurons but suppressed a-VTA dopaminergic neurons. Conversely, ethanol (>21 mM) dose-dependently reduced the frequency of the GABAergic spontaneous inhibitory postsynaptic currents (sIPSCs) generated by inhibitory neuronal firing but not miniature inhibitory postsynaptic currents (mIPSCs) in p-VTA dopaminergic neurons. By contrast, ethanol increased the frequency and amplitude of both sIPSCs and mIPSCs in a-VTA dopaminergic neurons. All of these effects of ethanol were abolished by a GABA$_A$ receptor antagonist. There was a strong negative correlation between ethanol-evoked modulation of sIPSCs and neuronal firing in VTA dopaminergic neurons. These results indicate that GABAergic inputs play an important role in ethanol's actions in the VTA. The differential effects of ethanol on sIPSCs and neuronal firing in the p-VTA and a-VTA could be the basis for ethanol reinforcement via the p-VTA.

Introduction

The ventral tegmental area (VTA) has posterior (p-VTA) and anterior (a-VTA) portions (Ikemoto, 2007), which may play different roles in drug reinforcement. Rodents learn to self-administer into p-VTA ethanol (EtOH) (Rodd-Henricks et al., 2000) and its metabolites such as acetaldehyde (Rodd et al., 2005a). Although blocking GABA$_A$ receptors in the a-VTA increases dopamine levels in the nucleus accumbens (NAcc) of rats (Ikemoto et al., 1997a; Ding et al., 2009), and rats self-administer a GABA$_A$ receptor antagonist into the a-VTA (Ikemoto et al., 1997b), they do not self-administer EtOH into the a-VTA (Rodd-Henricks et al., 2000; Rodd et al., 2005b,2008). Therefore, the a-VTA may not participate in self-reinforcing EtOH consumption.

Activation of VTA dopaminergic (DA) neurons is one of the cellular bases for EtOH reinforcement (Brodie et al., 1990,1999; Xiao et al., 2007, 2009). EtOH may stimulate DA neurons directly (Brodie et al., 1990, 1999), but there is increasing evidence that EtOH may activate DA neurons indirectly (Gallegos et al., 1999; Stobbs et al., 2004; Xiao et al., 2007, 2009; Xiao and Ye, 2008). Because VTA DA neurons are controlled by GABAergic inhibition (Johnson and North, 1992a; Xiao et al., 2007; Tan et al., 2010), modulation of GABAergic inputs could be an important mediator of EtOH's action on VTA DA neurons. We and others have found that EtOH inhibits VTA GABAergic neurons (Gallegos et al.,

ABBREVIATIONS: VTA, ventral tegmental area; a-VTA, anterior VTA; p-VTA, posterior VTA; DA, dopaminergic; DAMGO, [D-Ala2,*N*-Me-Phe4,Gly5-ol]enkephalin; MOR, μ-opioid receptor, NAcc, nucleus accumbens; TH, tyrosine hydroxylase; IPSC, inhibitory postsynaptic current; sIPSC, spontaneous IPSC; mIPSC, miniature IPSC; TTX, tetrodotoxin; ACSF, artificial cerebrospinal fluid; PBS, phosphate-buffered saline; TBS, Tris-buffered saline; EtOH, ethanol; SR-95531, 2-(3-carboxypropyl)-3-amino-6-(4 methoxyphenyl)pyridazinium bromide; K-S, Kolmogorov-Smirnov.

1999; Stobbs et al., 2004; Xiao et al., 2007). We further demonstrated that EtOH reduces action potential-dependent, GABA-mediated IPSCs recorded in VTA DA neurons, and that the EtOH-induced excitation of VTA DA neurons is attenuated by a GABA$_A$ receptor blocker or a saturating concentration of an antagonist or agonist of μ-opioid receptors (MORs) (Xiao et al., 2007; Xiao and Ye, 2008). These results support the notion that EtOH stimulates VTA DA neurons at least partly via MOR-mediated disinhibition. Under some conditions, EtOH was also reported to enhance spontaneous GABA release in VTA: 1) when endogenous opioidergic activity was negligible (Theile et al., 2008); 2) when neuronal firing was blocked (Theile et al., 2008, 2009), and 3) when GABAergic neurons were silenced by a MOR agonist (Xiao and Ye, 2008). These findings further indicate a pivotal role of opioids in the disinhibition of VTA DA neurons by EtOH.

Because p-VTA but not a-VTA DA neurons participate in EtOH reinforcement, we hypothesized that DA neurons in the a-VTA and p-VTA respond differently to EtOH. In the current study, we performed patch-clamp recordings in midbrain slices and found that EtOH has opposite effects on a-VTA DA and p-VTA neurons.

Materials and Methods

All procedures were approved by the Institutional Animal Care and Use Committee of the University of Medicine and Dentistry of New Jersey in accordance with the guidelines of the National Institutes of Health's *Guide for the Care and Use of Laboratory Animals* (Institute of Laboratory Animal Resources, 1996), minimizing the number of animals and their suffering. Experiments were done on slices from adolescent Sprague-Dawley rats (Taconic, Georgetown, NY) on postnatal days 22 to 32.

Slice Preparation. The midbrain slices were prepared as described earlier (Xiao et al., 2007; Xiao and Ye, 2008). Rats were anesthetized with ketamine/xylazine and then decapitated. Coronal midbrain slices (250–300 μm thick) were cut with a Compresstome VF-200 slicer (Precisionary Instruments, Greenville, NC) in ice-cold glycerol-based artificial cerebrospinal fluid (ACSF) containing 250 mM glycerol, 1.6 mM KCl, 1.2 mM NaH$_2$PO$_4$, 1.2 mM MgCl$_2$, 2.4 mM CaCl$_2$, 25 mM NaHCO$_3$, and 11 mM glucose and saturated with 95% O$_2$/5% CO$_2$ (carbogen) (Ye et al., 2006). In our experience, cutting slices in the low Na-glycerol medium enhances their viability and the quality of subsequent recordings. The slices were allowed to recover for at least 1 h in a holding chamber at 31°C in carbogen-saturated standard ACSF, which has the same composition as the glycerol-based medium, except that glycerol was replaced by 125 mM NaCl.

Electrophysiological Recording. Neurons in midbrain slices (Fig. 1) were visualized with an upright microscope (E600FN; Nikon, Melville, NY) and near-infrared illumination. Electrophysiological signals were obtained with MultiClamp 700 A amplifiers (Molecular Devices, Sunnyvale, CA), a Digidata 1320 A A/D converter (Molecular Devices), and pCLAMP 10.2 software (Molecular Devices). Data were filtered at 1 kHz and sampled at 5 kHz. The patch electrodes had a resistance of 4 to 6 MΩ when filled with a solution containing 135 mM K-gluconate, 5.0 mM KCl, 2.0 mM MgCl$_2$, 10.0 mM HEPES, 2.0 mM Mg ATP, and 0.20 mM GTP, and pH was adjusted to 7.2 with Tris base (for recordings of action potentials) or 135 mM KCl, 12 mM NaCl, 0.50 mM EGTA, 10 mM HEPES, 2.0 mM Mg-ATP, and 0.30 mM Tris-GTP, and pH adjusted to 7.3 with KOH (for recordings of sIPSCs). A single slice was transferred to a 0.30-ml recording chamber, where it was held down by a platinum ring and continually superfused with carbogenated ACSF (1.5–2.0 ml/min). The fact that 10 μM gabazine blocked most of GABAergic IPSCs within 90 s is an indication of the effective bath exchange time.

Spontaneous discharges of VTA DA neurons were recorded by the loose-patch cell-attached technique, which permits long-lasting recordings without perturbing the cytoplasmic contents. In some experiments, firing was recorded in whole-cell mode, in which the resting membrane potential and input resistance and synaptic currents could be measured. The slow firing of DA neurons allowed us to estimate the resting membrane potential that lies between the action potential threshold and after-hyperpolarization (Grace and Onn, 1989). After 10 min of stable baseline recordings, drugs were applied in the perfusate for 8 to 15 min, and then washed out for 10 min. All experiments were done at a temperature of 32 ± 1°C, maintained by an automatic temperature controller (Warner Instruments, Hamden, CT). Access resistance was monitored throughout: if it changed by >20% at any time during the experiments, the data were excluded.

Putative DA neurons were identified by their slow and regular firing rate, their depression by dopamine, the broad action potentials recorded in cell-attached mode, and the presence of a large hyperpolarization-activated inward current, I_h (Johnson and North, 1992b), recorded immediately after break-in. Although expression of I_h alone may not be sufficient to identify DA cells unequivocally (Margolis et al., 2006a), I_h is present in 84% of VTA DA neurons (Sarti et al., 2007), whereas GABAergic neurons do not have I_h (Margolis et al., 2006a). Thus, most I_h-positive neurons were probably DA neurons.

Immunocytochemistry. To validate the electrophysiological and pharmacological identification of DA neurons, a subset of neurons was examined immunocytochemically for tyrosine hydroxylase (TH; the rate-limiting enzyme for dopamine synthesis, a DA neuronal marker) as described previously (Xiao et al., 2009). In brief, we included Alexa Fluor 555 dextran (0.05%, w/v; Invitrogen, Carlsbad, CA) in the intrapipette solution to label the recorded neurons (red fluorescence in Fig. 2A). After electrophysiological recording, the slices were fixed for 2 h in 4% paraformaldehyde in PBS, washed twice with PBS, stored at 4°C in PBS and 0.1% sodium azide, and made ready for the immunohistochemical detection of TH. They were then permeabilized for 20 min in TBS/0.5% Triton X-100, blocked for 1 h in 5% donkey serum in TBS/0.1% Triton X-100, and incubated overnight at 4°C with a primary antibody (rabbit anti-TH; Pel-Freez Biologicals, Rogers, AR; 1:100 dilution) in TBS/0.1% Triton X-100 containing 5% donkey serum. The slices were then washed three times (5 min each) with TBS/0.1% Triton X-100, incubated for 1 h in secondary antibody at room temperature (Alexa Fluor 488 goat anti-rabbit IgG; Invitrogen; 1:500 dilution) in TBS/0.1% Triton X-100 containing 5% donkey serum, washed three times (10 min each) with TBS/0.1% Triton X-100, and then covered in Vectashield mounting medium with coverslips. The slides were immediately examined with a three-color immunofluorescence microscope (Nikon). TH-positive neurons were stained green (Fig. 2A).

Chemicals and Applications. 2-(3-Carboxypropyl)-3-amino-6-(4 methoxyphenyl)pyridazinium bromide (SR-95531; gabazine), dopamine, [D-Ala2,*N*-Me-Phe4,Gly5-ol]enkephalin (DAMGO), tetrodotoxin (TTX), and other chemicals were obtained from Sigma-Aldrich (St. Louis, MO). EtOH (95%; prepared from grain) was from Pharmco (Brookfield, CT) and stored in glass bottles. Chemicals were added in known concentrations to the superfusate. EtOH was perfused into the chamber for 8 to 10 min to ensure that measurements were made after the EtOH concentration stabilized in the tissue and the peak effect was attained (Appel et al., 2003). Owing to the volatility of EtOH, its actual tissue concentrations may be somewhat below the stated values. However, because of the fast perfusion (2 ml/min) and small recording chamber (0.30 ml), we are confident that the concentrations reported below are close to the final bath concentrations. The behaviorally active range for blood EtOH concentrations in the rat extends from 40 mM (sedation) to 90 mM (loss of righting reflex) (Majchrowicz and Hunt, 1976). Rats self-administer 44 to 55 mM EtOH directly into the VTA, indicating that these concentrations of EtOH cause reinforcement in vivo (Rodd-Henricks et al., 2000).
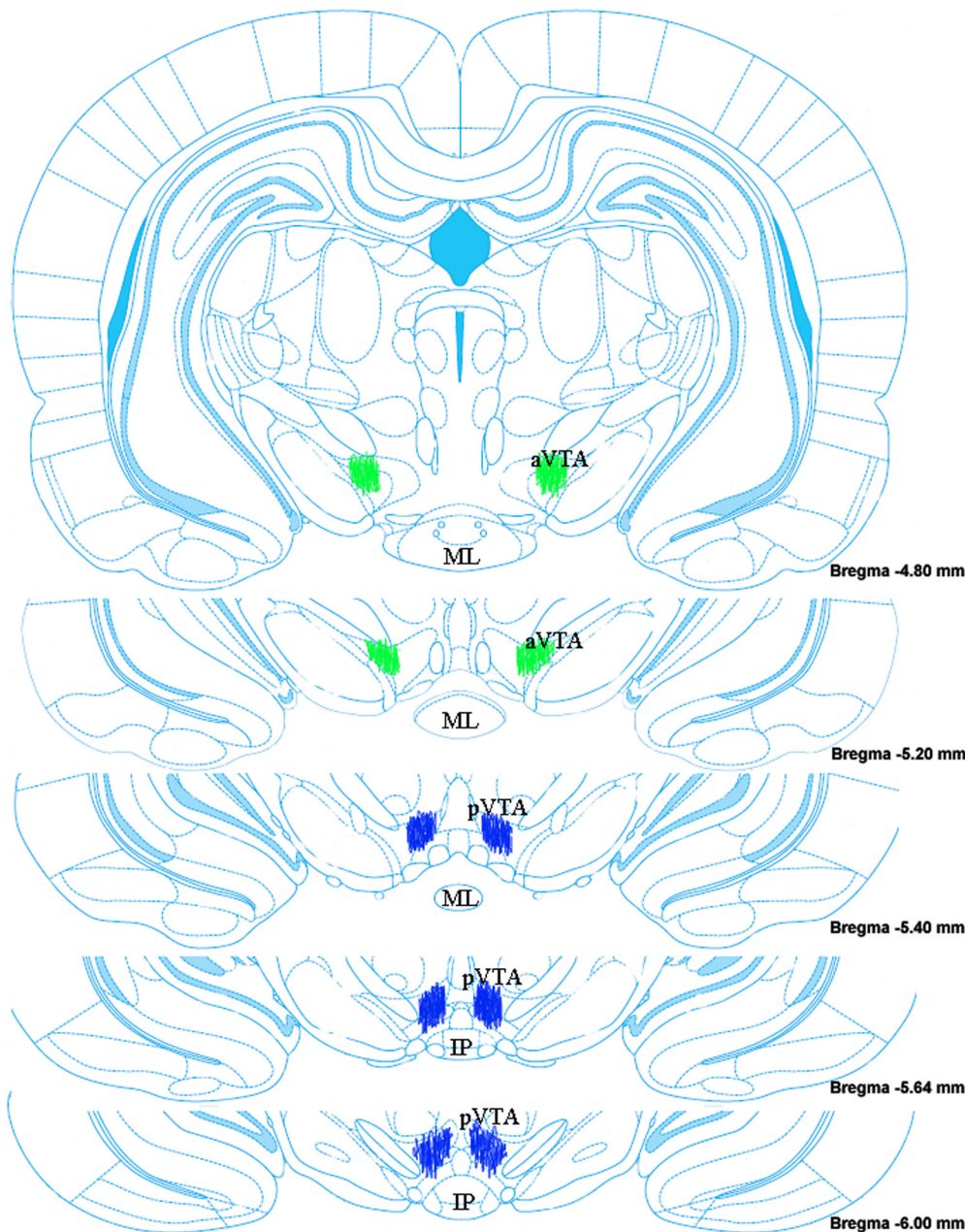
Fig. 1. Coronal rat brain sections containing the a-VTA or p-VTA. Green spots indicate locations of the recordings in the a-VTA (−4.8 to −5.3 mm from bregma) and blue sports indicates locations in the p-VTA (−5.4 to −6.2 mm from bregma). Adapted from Paxinos and Watson (2007).

Data Analysis. Electrophysiological data were analyzed with Clampfit 10.2 (Molecular Devices). Action potentials were detected with a threshold detection protocol in Clampfit. The firing rate was calculated over 1-min intervals immediately before and during drug administration, and peak effects were expressed as percentage change from control. sIPSCs were screened automatically by a template with a threshold of 10 pA. They were then visually inspected and accepted or rejected on the basis of their time course: rise times 0.2 to 6.3 ms and decay times 0.2 to 20.1 ms. The sIPSC frequency during a 2-min interval at the peak of the drug response was normalized to the control value measured during a 5-min period before drug application. Drug effects are given as mean percentage changes (± S.E.M.). Their statistical significance was assessed with the two-tailed paired t test. For tests of several drug concentrations or more than one drug, an appropriate one- or two way analysis of variance was applied, followed by Student-Newman-Keuls post hoc comparisons when needed. Statistical analyses were performed with Sigma-Plot (SPSS Inc., Chicago, IL). Dose-response data (in Fig. 3D) were fitted to the logistic equation: $y = 100x^a/(x^a + x_o^a)$, where y is the percentage change, x is the concentration of EtOH, a is the slope parameter, and x_0 is the EtOH concentration that induces a half-maximal change. To determine whether the effects of EtOH on sIPSC frequency and the firing rate of DA neurons are correlated, these data were plotted and then fitted with a linear equation ($y = a + bx$), as illustrated in Fig. 7D.

Results

Definition of the a-VTA and p-VTA

The locations of recording sites in the VTA are indicated in Fig. 1, where the a-VTA, the antereomedial or lateral VTA extends from 4.8 to 5.2 mm posterior to bregma, and the p-VTA, the posteromedial VTA extends from 5.3 to 6.0 mm posterior to the bregma, in accordance with previous studies (Ikemoto et al., 1997a; Rodd-Henricks et al., 2000). The figure is not a quantitative representation of all of the placements of recording electrodes.

a-VTA DA neurons

A **a** Alexa FluoR 555   **b** TH Positive   **c** Merged
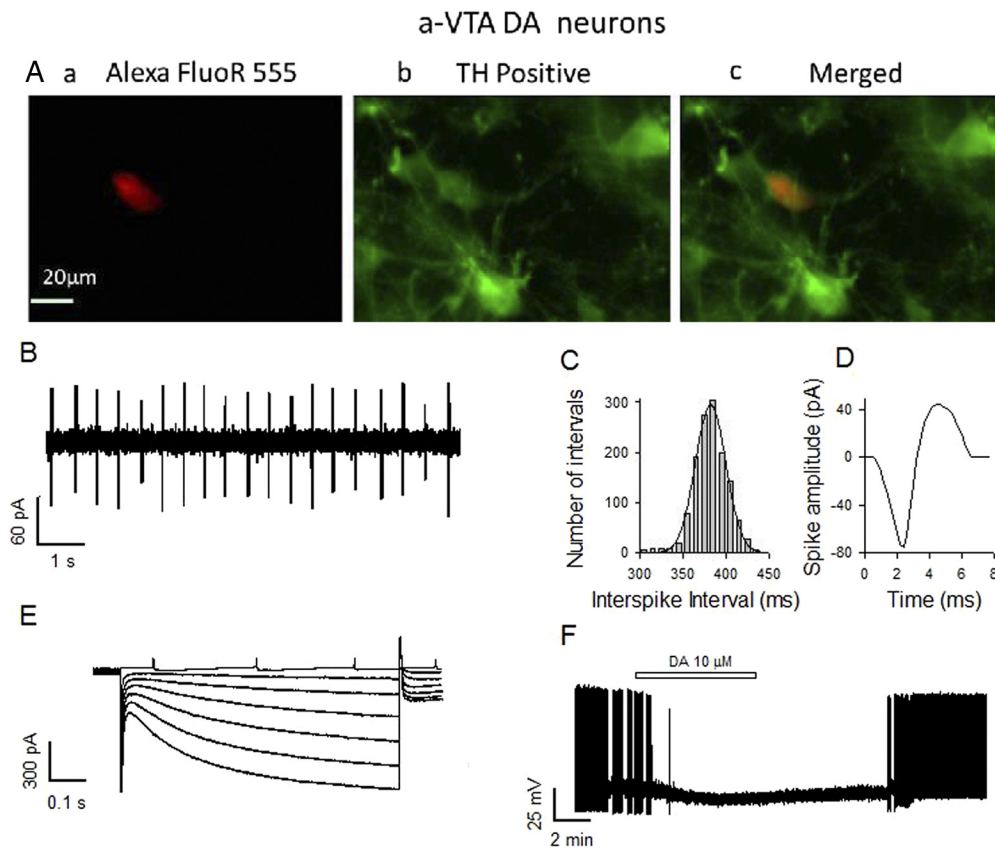
Fig. 2. Properties of DA neurons in the a-VTA. A, typical neuron labeled with Alexa FluoR 555 Dextran (a; red) is also TH-positive (b; green), and two images are overlaid (c). B to D, typical DA neuron showing regular pacemaker firing (B), histogram of interspike intervals (C), and broad spike (D). The spikes were recorded by a cell-attached patch-clamp technique. E, in voltage-clamp mode, a series of hyperpolarizing steps (from a holding potential of −50 mV to −110 mV in 10-mV increments) elicited prominent I_h-like inward current relaxation. F, characteristic inhibition of spontaneous firing by 10 μM dopamine, recorded by whole-cell current clamp.

Comparison of Properties of DA Neurons in the a-VTA and p-VTA

We tested the electrophysiological and pharmacological properties of a-VTA and p-VTA neurons. We first recorded the spontaneous firing of VTA neurons by the cell-attached patch-clamp method (Fig. 2B) and then made whole-cell recordings. To elicit I_h, we applied a series of hyperpolarizing steps between −60 and −110 mV (in increments of 10 mV) from a holding potential of −60 mV and measured the resulting inward currents (Fig. 2E). To monitor membrane input resistance, we applied 400-ms × 5-mV hyperpolarizing steps, from a holding potential of −60 mV, and calculated the resistance by Ohm's law (data not shown). In addition, we made current clamp recordings from some neurons and measured the peak amplitude of spikes (Fig. 2F).

We first confirmed that I_h and inhibition by dopamine can effectively identify the DA nature of VTA neurons. As described under *Materials and Methods*, we labeled 13 recorded neurons with Alexa 555 and did TH antibody staining to identify these neurons (Fig. 2A). We found that 1) 12/13 of I_h-positive neurons expressed TH; 2) 11/12 of TH-positive neurons showed I_h-like inward slow relaxations, which were absent in TH-negative neurons; and 3) 10 μM dopamine depressed or blocked the ongoing firing of 9/11 TH-positive neurons, probably by activating D_2-like dopamine receptors (Fig. 2F).

We detected I_h in both a-VTA (50/60) and p-VTA (50/54) neurons. The I_h-positive neurons fired slowly and regularly and had wide spikes (Fig. 2, B-D). We did not observe significant differences between a-VTA and p-VTA neurons in firing rate, spike width, and input resistance, except that the peak amplitude of I_h and gabazine effect seemed smaller than that

of the p-VTA (Table 1). As illustrated in Fig. 2F and Table 1, 10 μM dopamine blocked the discharge and/or caused a similar hyperpolarization of TH-positive neurons in both the a-VTA and p-VTA. Thus, the properties of a-VTA and p-VTA DA neurons were comparable with those of VTA DA neurons in general, as described previously (Yim and Mogenson, 1980; Brodie et al., 1990, 1999; Johnson and North, 1992a; Xiao et al., 2007, 2009).

DA Neuronal Firing Was Enhanced by EtOH in the p-VTA but Depressed in the a-VTA

We tested the effect of EtOH on a-VTA or p-VTA DA neurons. We defined the effects of EtOH on VTA DA neurons in slices as facilitation or inhibition when EtOH (>40 mM) changed firing rate by >10%.

p-VTA. In agreement with previous reports (Brodie et al., 1990, 1999; Xiao et al., 2007, 2009), in the p-VTA, EtOH (43 and 86 mM) facilitated the firing of 42/52 of p-VTA DA neurons (Fig. 3B1) and reduced that of 6/52 or had no effect on 4/52 DA neurons (Fig. 3C). As illustrated in Fig. 3B2, EtOH (21 and 86 mM) increased the firing rate of p-VTA cells gradually. The effect reached a steady level 5 to 10 min after the start of EtOH application and diminished rapidly during EtOH washout. The concentration dependence of this effect of EtOH (21–120 mM), shown in Fig. 3D, was well fitted by a logistic equation ($r^2 = 0.97$), giving an EC_{50} of 34.1 ± 0.6 mM and a maximal effect of 43.1 ± 0.5%.

a-VTA. In contrast, EtOH (21–86 mM) suppressed the firing of 35/60 of a-VTA DA neurons and increased the firing of only 15/60 or had no effect on 10/60 of neurons (Fig. 3, A1, A2, and C). The EtOH-induced inhibition developed steeply, between 5 to 10 min after the start of EtOH application (Fig.
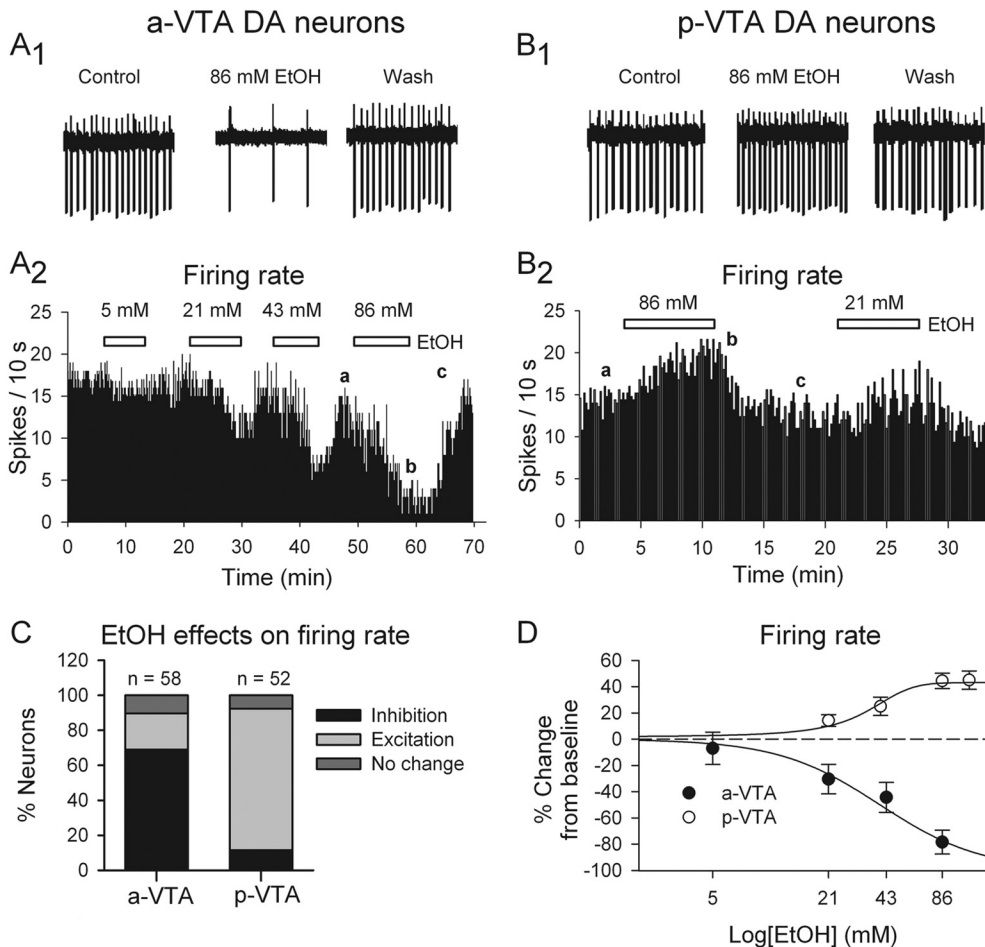
Fig. 3. Opposite effects of EtOH on spontaneous firing in a-VTA and p-VTA DA neurons. A1 and B1, traces recorded in the a-VTA (A1) and p-VTA (B1) before (Control), during (86 mM EtOH), and after (Wash) the application of EtOH. A2 and B2, histograms show the concentration-dependent depression of firing of one a-VTA DA neuron (A2) and increase in the firing of a p-VTA DA neuron (B2). EtOH concentrations are as indicated. C, stacked bar charts of percentage of DA neurons inhibited (black), excited (gray), or unaffected (dark gray) by EtOH (≥ 43 mM) in the a-VTA and p-VTA. D, concentration dependence of EtOH effects on the firing of DA neurons in the a-VTA ($\bullet$) and p-VTA ($\circ$). EC$_{50}$ or IC$_{50}$ was 34.1 ± 0.6 or 39.7 ± 1.5 mM, respectively. Note: only those neurons responding with inhibition in the a-VTA and excitation in the p-VTA were used for the analysis.

TABLE 1

Electrophysiological and pharmacological properties of a-VTA and p-VTA DA neurons

	a-VTA		p-VTA	
	Mean $\pm$ S.E.M.	n	Mean $\pm$ S.E.M.	n
10 μM DA-induced V_m change, mV	-6.8 ± 1.1	9	-7.8 ± 2.1	10
Ongoing firing, Hz	1.2 ± 0.3	56	1.3 ± 0.3	56
Current spike width, ms	3.8 ± 0.8	50	2.2 ± 0.7	47
Peak I_h, pA	169 ± 11	62	107 ± 18	68
Action potential amplitude, mV	64 ± 3	25	65 ± 4	5
Resting membrane potential, mV	-52.6 ± 3.2	5	-50.5 ± 1.8	6
Gabazine-induced change in firing rate, %	29 ± 11	15	47 ± 17	14

3A2); because firing recovered almost completely after 5-min washout (Fig. 3, A1 and A2), we could test several concentrations of EtOH on the same neuron. Because the effects of single and multiple exposures of EtOH were similar, we pooled all of the data. The concentration dependence of EtOH-induced inhibition in the a-VTA (shown in Fig. 3D) was also well fitted by a logistic equation ($r^2 = 0.99$), giving an IC$_{50}$ of 39.7 ± 1.5 mM and a maximal effect of $100 \pm 4\%$. In addition, we noted that 86 mM EtOH significantly hyperpolarized a-VTA DA neurons (by -3.9 ± 0.8 mV; $n = 20$; $p < 0.05$, traces not shown, but see Fig. 7C).

GABA Release Was Enhanced by EtOH in the a-VTA and Reduced in the p-VTA

We next asked whether EtOH might have different effects on GABAergic inputs to a-VTA and p-VTA DA neurons. To answer this question, we examined the effects of EtOH on sIPSCs in DA neurons in the a-VTA and p-VTA, while recording at a holding potential of -65 mV in whole-cell patch-clamp mode. We added to the perfusate 6,7-dinitroquinoxaline-2,3-dione (20 μM), a non-N-methyl-D-aspartate receptor antagonist, and DL-2-amino-5-phosphono-valeric acid (50 μM), a N-methyl-D-aspartate receptor antagonist, to block the ionotropic glutamate receptors that mediate spontaneous excitatory postsynaptic currents. The remaining inhibitory postsynaptic currents (sIPSCs) were eliminated by gabazine (10 μM), indicating that they were indeed mediated by GABA$_A$ receptors (data not shown).

In a-VTA. EtOH (≥ 21 mM) significantly accelerated sIPSC frequency in DA neurons. The frequency rose quickly, remained high during the application of EtOH, and fell rapidly to the baseline after its washout (Fig. 4A). The effect increased with EtOH concentrations, giving a concentration-response relation that was well fitted by a logic equation

IPSCs in a-VTA DA neurons
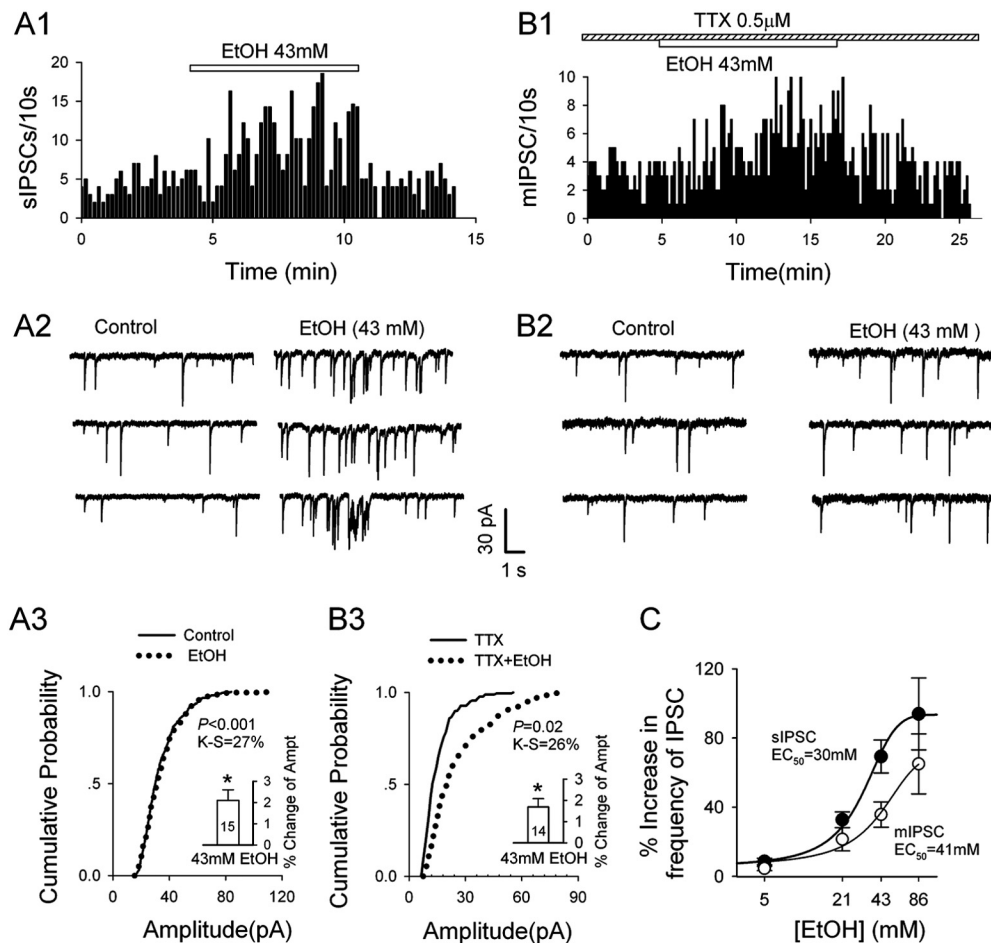
Fig. 4. EtOH enhanced mIPSC and sIPSC frequency in a-VTA DA neurons. A1 and A2, representative histogram (A1) and traces (A2) show EtOH-induced increase in sIPSC frequency. A3, cumulative probability plots show little effect of EtOH on sIPSC amplitude. Inset is the mean ± S.E.M. of data from 15 cells. B1 and B2, representative histogram (B1) and traces (B2) showing EtOH-induced increase in mIPSC frequency. B3, cumulative probability plots indicate a robust increase in mIPSC amplitude. Inset is the mean ± S.E.M. of data from 15 cells. C, concentration dependence of EtOH facilitation (percentage increase) of frequency of sIPSCs and mIPSCs. For all concentrations, $n = 8$–12 neurons. EC_{50} was 30 ± 3 mM for sIPSCs and 41 ± 4 mM for mIPSCs.

($r^2 = 0.99$). The estimated EC_{50} was 30 ± 3 mM and the maximum at $94 \pm 6\%$ (Fig. 4C). A K-S test of individual cells showed excellent agreement between control and EtOH values of sIPSC amplitudes, except for some very large sIPSCs induced by EtOH (Fig. 4A3), most likely caused by overlapping of some events at high frequencies. In support of the latter possibility, EtOH had no significant effect on the kinetics of sIPSCs (data not illustrated).

We next added 0.5 to 1 µM tetrodotoxin (TTX) to the perfusate to block action potential-dependent neurotransmitter release so that we could examine the effects of EtOH (21–86 mM) on miniature IPSCs (mIPSCs). As illustrated in Fig. 4, B1 to B3 and C, 21, 43, and 86 mM EtOH significantly and concentration-dependently increased mIPSC frequency. The effects were reversible after EtOH washout (Fig. 4B1). These results are consistent with previous studies (Theile et al., 2009). A K-S test of individual cells showed that EtOH systematically increased the amplitude of mIPSCs (Fig. 4B3). Such an increase in amplitude suggests a change in postsynaptic receptors, although EtOH had no significant effect on the kinetics of mIPSCs (data not illustrated).

In p-VTA. EtOH (> 43 mM) had the opposite effects on sIPSCs of DA neurons (Fig. 5, A1-A4 and B1-B4). EtOH dose-dependently lowered sIPSC frequency: 5, 21, 43, and 86 mM EtOH reduced sIPSC frequency by $2.2 \pm 1.1\%$ ($n = 8$; $P > 0.05$), $9.3 \pm 2.5\%$ ($n = 8$; $p < 0.05$), $33.4 \pm 4.1\%$ ($n = 8$; $p < 0.01$), and $35.4 \pm 4.5\%$ ($n = 8$; $p < 0.01$), respectively (Fig.

5A5). A K-S test of individual cell shows that EtOH significantly lowered the incidence of large sIPSCs, probably owing to reduced overlap (Fig. 5A3; note inset histogram). However, mIPSCs recorded in the presence of TTX showed no significant effect of EtOH (43 mM) (Fig. 5, B1-B4).

### Activation of MORs Inhibited GABA Release More Potently in the p-VTA than the a-VTA

There is morphological and molecular evidence that more MORs are present in the p-VTA then the a-VTA (Mansour et al., 1994, 1995), possibly accounting for the observed differential EtOH effects in the p-VTA versus the a-VTA. To further test this possibility, we compared the effect of DAMGO, the MOR agonist, on sIPSCs in the DA neurons of the a-VTA and p-VTA (Fig. 6). DAMGO (1 µM) suppressed sIPSC frequency in a-VTA DA neurons by $28.9 \pm 5.6\%$ ($n = 7$; $p < 0.05$) which is significantly less ($t = 2.845$; $p = 0.017$; unpaired t test) than $42.2 \pm 10.6\%$ ($n = 5$; $p = 0.02$), their depression in the p-VTA. DAMGO (1 µM) had no significant effect on the amplitude of sIPSCs in both the a-VTA ($n = 7$; $p = 0.58$) and the p-VTA ($n = 5$; $p = 0.24$).

EtOH Inhibited a-VTA DA Neurons through a GABAergic Pathway

To test whether increased GABA release contributes to the EtOH-induced inhibition of a-VTA DA neurons, we compared the effects of EtOH on DA neuronal firing in the absence and
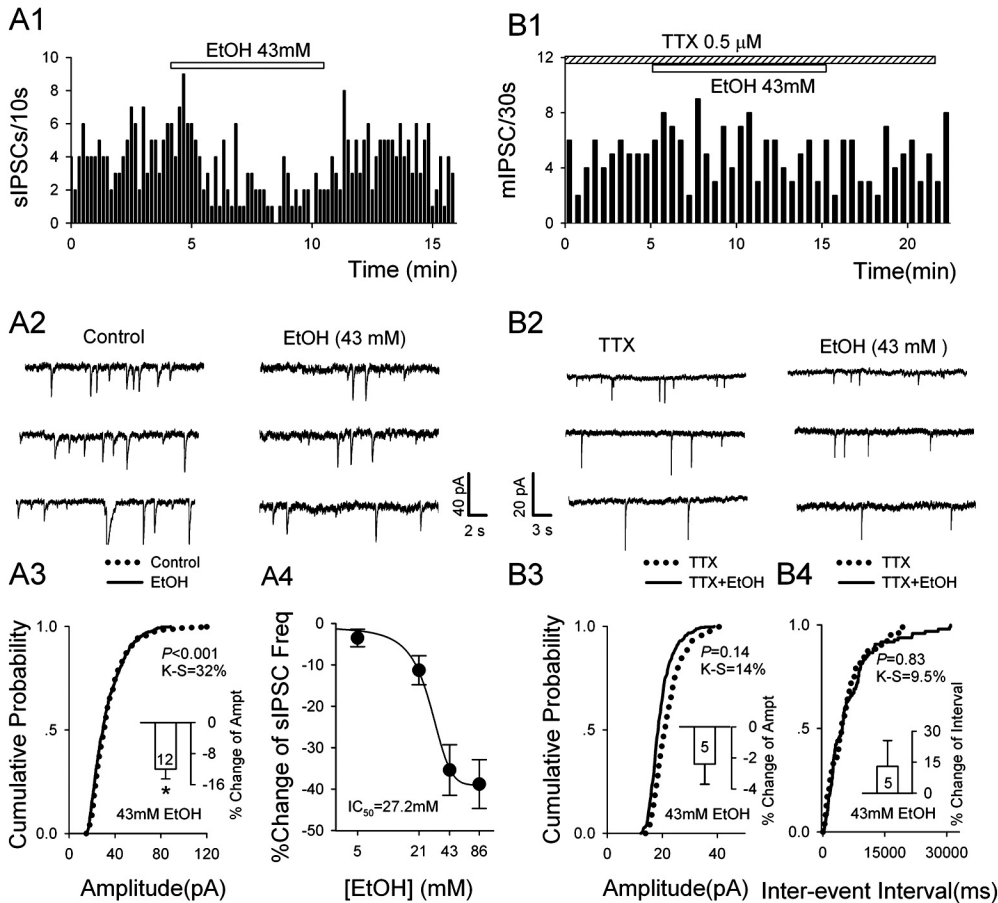
Fig. 5. EtOH reduced frequency of sIPSCs in p-VTA DA neurons. A1 and A2, time course (A1) and traces (A2) show reversible depression of sIPSC frequency by 43 mM EtOH. A3, cumulative probability plots indicate minimal changes in sIPSC amplitude. Inset is the mean ± S.E.M. of data from 12 cells. *, $P < 0.05$, compared with control. A4, concentration dependence of EtOH suppression (percentage of decrease) of frequency of sIPSCs. B1 and B2, time course (B1) and traces (B2) show that 43 mM EtOH had no significant effect on mIPSC frequency. B3 and B4, cumulative probability plots indicate that EtOH had no significant effect on mIPSC frequency and amplitude. Insets are the mean ± S.E.M. of data from five cells.

presence of gabazine. EtOH (86 mM) caused a robust inhibition of a-VTA DA neurons (by $77 \pm 12\%$; $n = 18$; $p < 0.01$) (Fig. 7, A and B). Gabazine (10 μM) alone significantly increased the basal firing rate in a-VTA DA neurons by $29 \pm 11\%$ ($n = 15$; $p < 0.05$), indicating some tonic GABAergic input. From the newly established baseline (in 10 μM gabazine), EtOH (86 mM) failed to inhibit DA neurons: firing changed by only $10 \pm 11\%$ ($n = 15$; $p = 0.371$) (Fig. 7, A and B). This is significantly less than EtOH's effect in the absence of gabazine (one-way analysis of variance; $p = 0.003$; $F = 16.894$; df = 3). In some neurons, we recorded neuronal firing in the whole-cell current clamp mode, in which we could measure membrane potential changes upon drug application. EtOH (86 mM) caused a membrane hyperpolarization by 4.8 ± 0.8 mV ($n = 15$; $p < 0.05$). In the presence of 10 μM gabazine, EtOH's effect on the membrane potential vanished (-0.37 ± 0.38 mV; $n = 10$; $p = 0.19$) (Fig. 7C).

After pooling all of the effects of various concentrations of EtOH on DA neuron firing rate and sIPSC frequency, from both the a-VTA and p-VTA, we plotted mean changes in firing rate against corresponding mean changes in sIPSC frequency (Fig. 7D). The slope of the best-fitting line was very close to -1.0 ($r = 0.991$; $p < 0001$), indicating that, within this range of EtOH concentrations, the firing rate was inversely proportional to sIPSC frequency, in keeping with the idea that EtOH-induced changes in the firing rate of DA neurons are mediated principally by changes in GABAergic input.

Discussion

DA Neurons of the p-VTA and a-VTA Have Similar Properties.
Few electrophysiological studies have separately characterized neurons in the a-VTA and p-VTA. We found that DA neurons in the a-VTA and p-VTA in general have similar electrophysiological and pharmacological properties: a broad spike (~3.5 ms), slow pacemaker firing (~1.2 Hz), a prominent I_h, and inhibition and/or hyperpolarization by dopamine (Fig. 2). By these criteria, most of the recorded VTA neurons were probably dopaminergic. Although this incidence is much higher than reported by some authors (Margolis et al., 2006b; Zhang et al., 2010), it is close to that observed in many other studies (Yim and Mogenson, 1980; Brodie et al., 1990, 1999; Johnson and North, 1992a; Xiao et al., 2007, 2009). This result also supports previous reports that few VTA neurons are GABAergic (Johnson and North, 1992a; Zhang et al., 2010). Although I_h has been used as an electrophysiological index of DA neurons in the VTA (Johnson and North, 1992a; Pidoplichko et al., 1997; Thomas et al., 2000; Wooltorton et al., 2003), only a small or no I_h is observed in the medial VTA DA neurons (Zhang et al., 2010) or the DA neurons projecting to limbic areas (Ford et al., 2006; Lammel et al., 2008). VTA DA neurons projecting to the prefrontal cortex express low levels of D_2-like dopamine receptors (Lammel et al., 2008). These neurons are also located in the medial part of the VTA (Ikemoto, 2007). Most of the neurons we recorded from the a-VTA were in its lateral part.

a-VTA

p-VTA

A1 Control   DAMGO

B1 Control   DAMGO

20 pA | 10 s

A2

C

B2
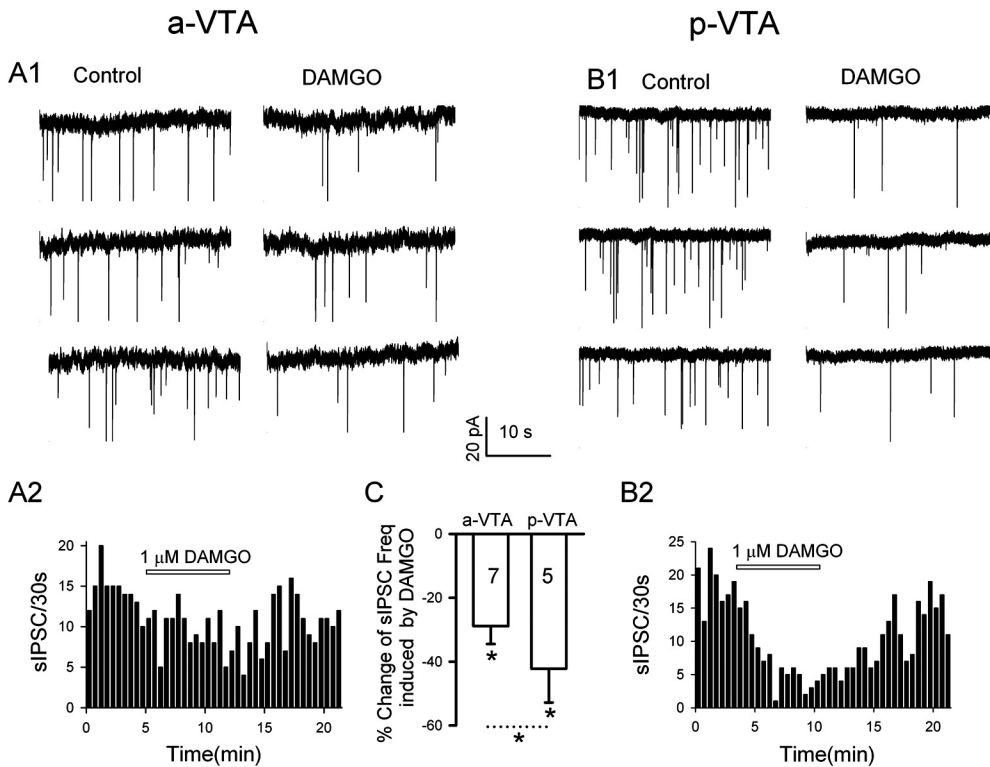
Fig. 6. Activation of MORs inhibited GABA release more potently in the p-VTA than the a-VTA. A1 and A2, traces (A1) and time course (A2) show reversible depression of sIPSC frequency by 1 μM DAMGO in the a-VTA. B1 and B2, traces (B1) and time course (B2) show reversible depression of sIPSC frequency by 1 μM DAMGO in the p-VTA. C, mean ± S.E.M. of data from seven (a-VTA) and five (p-VTA) cells show a significant difference between DAMGO's inhibition of sIPSC frequency of a-VTA and p-VTA DA neurons. ∗, $P < 0.05$, compared with control or between a-VTA and p-VTA, as indicated.

EtOH Differentially Stimulated and Inhibited DA Neurons in the p-VTA and a-VTA. Acute EtOH accelerates the firing of DA neurons in VTA in vivo (Gessa et al., 1985), in brain slices (Brodie et al., 1990; Xiao et al., 2007, 2009), and in isolated neurons (Brodie et al., 1999). However, those previous studies did not discriminate between EtOH's actions in the p-VTA and a-VTA. Because EtOH has reinforcing effects in vivo only when injected into the p-VTA, one could expect that EtOH acts differently in the a-VTA and p-VTA. Indeed, as we show here for the first time, EtOH (≥21 mM) stimulates most p-VTA DA neurons, but inhibits many a-VTA DA neurons (Fig. 3). That these findings are reliable is confirmed by the reversibility, concentration dependence, and reproducibility of the observed changes. Although EtOH concentrations causing half-maximal effects in a-VTA and p-VTA neurons were similar (34 versus 39 mM), the maximal inhibition of a-VTA DA neurons was especially striking. This suggests that the opposite effects of EtOH observed in a-VTA and p-VTA DA neurons might be mediated by different mechanisms or pathways. The inhibitory effects of EtOH on a-VTA DA neurons were also manifested by a robust membrane hyperpolarization, presumably caused by increased GABAergic inhibition, possibly reinforced by EtOH-induced sensitization of extrasynaptic GABA receptors. DA neurons in the p-VTA and a-VTA project to different subregions of the NAcc (Ikemoto, 2007). Most p-VTA DA neurons, but only a small fraction of a-VTA DA neurons, project to the ventromedial part, and most a-VTA DA neurons innervate the lateral shell and core of the NAcc. The meso-ventromedial NAcc DA system predominantly mediates drug reward (Ikemoto, 2007). Our observation that EtOH stimulated >80% of p-VTA DA neurons, but only 25% of a-VTA DA neurons, is consistent with their differential projections and with the fact that EtOH's reinforcing effect is mediated primarily by p-VTA neurons (Rodd-Henricks et al., 2000; Rodd et al., 2005b, 2008).

EtOH Inhibited and Facilitated GABA Release in p-VTA and a-VTA DA Neurons, Respectively. The inhibitory inputs to VTA DA neurons largely originate from GABAergic neurons located in the VTA (Johnson and North, 1992b), but also from the NAcc (Waddington and Cross, 1978; Kalivas, 1993), the ventral pallidum (Walaas and Fonnum, 1980; Kalivas, 1993), and the rostromedial tegmental nucleus (Jhou et al., 2009). We still lack information about differences in the origins of GABAergic inputs to the a-VTA and p-VTA. In an in vivo microdialysis study, a-VTA DA neurons seemed to receive stronger GABAergic inputs than did p-VTA DA neurons (Ding et al., 2009).

A major finding of the current study is that EtOH inhibited ongoing synaptic GABA release in p-VTA DA neurons (Fig. 5), but facilitated such GABA release in a-VTA DA neurons (Fig. 4). The effects were reversible, concentration-dependent, and reproducible in the same neuron. This inhibition by EtOH is consistent with our previous observations (Xiao and Ye, 2008); but facilitation was reported in some other studies (Theile et al., 2008, 2009; Xiao and Ye, 2008). The VTA DA neurons in our previous study probably were located in the p-VTA, because we selected neurons stringently by such characteristics as disinhibition by MOR agonist, inhibition by 100 nM quinpirole, broad action potentials (half-width >1.2 ms), and expression of I_h (Xiao et al., 2007; Xiao and Ye, 2008). These criteria excluded a-VTA DA neurons that have lower levels of MORs (Mansour et al., 1994,1995). However, the neurons selected by the above-mentioned criteria account for only 50% of TH-positive neurons (Margolis et al., 2003; Xiao et al., 2009). Therefore, in this study, we used less stringent criteria and confirmed the neuronal identity by post hoc TH staining in some neurons (Fig. 2). We observed EtOH facilitation of both action potential-dependent and -independent GABA release in the a-VTA (Fig. 4). A similar effect was reported by Theile et al. (2008, 2009). It is note-

a-VTA
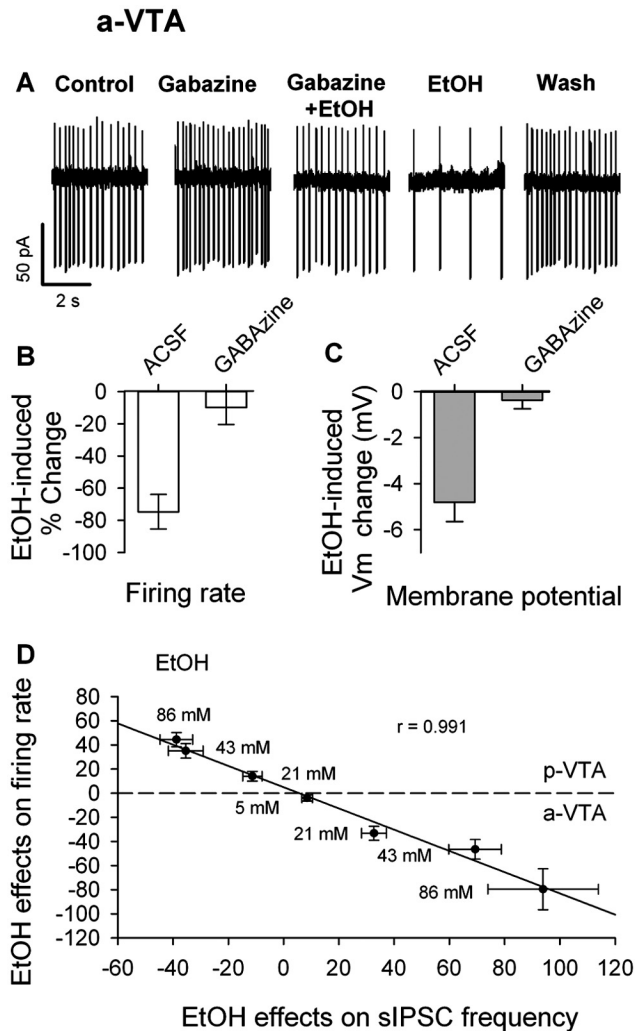
Fig. 7. Linear relationship between EtOH effects on sIPSCs and discharge of VTA DA neurons. A, traces from a-VTA DA cell show baseline firing (Control) and the effects of gabazine, gabazine and 86 mM EtOH (gabazine + EtOH), 86 mM EtOH (EtOH) alone, and after washout of all drugs (Wash). B, summary of inhibition of a-VTA DA neuron firing by EtOH (86 mM) in the absence (control; $n = 18$) and presence of 10 μM gabazine ($n = 15$). C, summary of membrane hyperpolarization of a-VTA DA neurons induced by EtOH (86 mM) in the absence (Control; $n = 18$) and presence of 10 μM gabazine ($n = 15$). D, scatter plot of EtOH effects on the discharge of both a-VTA and p-VTA DA neurons against EtOH's effects on sIPSC frequency. Each point corresponds to the effects of one concentration of EtOH on firing rate and sIPSC frequency. EtOH concentrations are indicated. The points above the dashed line are the averaged effects of EtOH on p-VTA DA neurons; those below the dashed line are the averaged effects of EtOH on a-VTA DA neurons. These points were fitted by a linear equation ($y = a + bx$), with a correlation coefficient of 0.991 ($P < 0.0001$).

worthy that those investigators reported EtOH-induced excitation of DA neurons with increased GABA release, suggesting that the EtOH-induced excitation of VTA DA neurons could also be mediated by other cellular mechanisms, including direct excitation (Brodie et al., 1999; Appel et al., 2003; Okamoto et al., 2006).

We earlier reported that when 3 μM DAMGO, a MOR agonist, silences VTA GABAergic neurons, the inhibitory action of EtOH (40 mM) on sIPSC frequency (by $-38 \pm 9\%$; $n = 5$) is reversed to facilitation ($57 \pm 10\%$; $n = 6$) (Xiao and Ye, 2008). Coincidentally, this facilitation (induced by 40 mM EtOH in the presence of DAMGO) is comparable with EtOH's

facilitating action on sIPSCs in a-VTA DA neurons (by $69 \pm 10\%$). We suggest that although EtOH tends to facilitate GABA release, this may be counterbalanced by enhanced opioidergic inhibition of GABA neurons. Because more MORs are expressed in the p-VTA than in the a-VTA, the opioidergic inhibition would more readily overcome the facilitation of GABA release in the p-VTA than in the a-VTA.

GABAergic Mechanisms Underlying Differential EtOH Effects in the VTA. In the a-VTA, there was a strongly negative correlation between sIPSCs and DA neuronal firing (Fig. 7D). The likelihood of cause-effect relationship between EtOH effects on GABA release and neuronal firing in VTA DA neurons was further supported by the suppression of EtOH's action when GABA$_A$ receptors were blocked by gabazine (Fig. 7, A-C, and Xiao et al., 2007).

Curiously, in the a-VTA, EtOH markedly enhanced the amplitude mIPSCs but not sIPSCs. A possible explanation for this seemingly paradoxical finding is that the ongoing quantal release does not activate the same postsynaptic receptors as the transmitter released by action potentials [as recently reported by Sara et al. (2011)]. Because both mIPSC and sIPSC frequency was also sharply enhanced, EtOH affects GABAergic transmission in the a-VTA by targeting both preterminal and terminal compartments, as well as by increasing the sensitivity of postsynaptic GABA$_A$ receptors to the agonist. Conversely, in the p-VTA the clearly predominant effect was the TTX-sensitive sIPSCs, suggesting that EtOH acts mainly by depressing the firing of the inhibitory neurons.

Further evidence in support of this conclusion is that in the VTA MORs are expressed mostly on the somata and dendrites of non-DA, presumably inhibitory, neurons (Mansour et al., 1994, 1995; Garzón and Pickel, 2001), with only 8% on inhibitory axonal terminals (Dilts and Kalivas, 1989; Garzón and Pickel, 2001). This suggests that μ-opioid actions on inhibitory inputs to VTA DA neurons in coronal slices are mediated principally by GABAergic neurons situated in the VTA (Johnson and North, 1992a). We did not study the mechanism by which EtOH facilitated GABA release in the current study. However, a previous study has suggested that this may involve activation of 5-hydroxytryptamine type 2C receptors (Theile et al., 2009).

Conclusion

For the first time we show that 1) EtOH stimulates p-VTA DA neurons, but inhibits a-VTA DA neurons; and 2) these effects seem to be mediated by a corresponding decrease or facilitation of GABA release, respectively. These findings could explain why rats self-administer EtOH into the p-VTA but not into the a-VTA (Rodd-Henricks et al., 2000).

References

Appel SB, Liu Z, McElvain MA, and Brodie MS (2003) Ethanol excitation of dopaminergic ventral tegmental area neurons is blocked by quinidine. *J Pharmacol Exp Ther* **306:**437–446.

Brodie MS, Pesold C, and Appel SB (1999) Ethanol directly excites dopaminergic ventral tegmental area reward neurons. *Alcohol Clin Exp Res* **23:**1848–1852.

Brodie MS, Shefner SA, and Dunwiddie TV (1990) Ethanol increases the firing rate of dopamine neurons of the rat ventral tegmental area in vitro. *Brain Res* **508:** 65–69.

Dilts RP and Kalivas PW (1989) Autoradiographic localization of μ-opioid and neurotensin receptors within the mesolimbic dopamine system. *Brain Res* **488:** 311–327.

Ding ZM, Liu W, Engleman EA, Rodd ZA, and McBride WJ (2009) Differential effects of dopamine D2 and GABA_A receptor antagonists on dopamine neurons between the anterior and posterior ventral tegmental area of female Wistar rats. *Pharmacol Biochem Behav* **92:**404–412.

Ford CP, Mark GP, and Williams JT (2006) Properties and opioid inhibition of mesolimbic dopamine neurons vary according to target location. *J Neurosci* **26:** 2788–2797.

Gallegos RA, Lee RS, Criado JR, Henriksen SJ, and Steffensen SC (1999) Adaptive responses of γ-aminobutyric acid neurons in the ventral tegmental area to chronic ethanol. *J Pharmacol Exp Ther* **291:**1045–1053.

Garzón M and Pickel VM (2001) Plasmalemmal μ-opioid receptor distribution mainly in nondopaminergic neurons in the rat ventral tegmental area. *Synapse* **41:**311–328.

Gessa GL, Muntoni F, Collu M, Vargiu L, and Mereu G (1985) Low doses of ethanol activate dopaminergic neurons in the ventral tegmental area. *Brain Res* **348:**201–203.

Grace AA and Onn SP (1989) Morphology and electrophysiological properties of immunocytochemically identified rat dopamine neurons recorded in vitro. *J Neurosci* **9:**3463–3481.

Ikemoto S (2007) Dopamine reward circuitry: two projection systems from the ventral midbrain to the nucleus accumbens-olfactory tubercle complex. *Brain Res Rev* **56:**27–78.

Ikemoto S, Kohl RR, and McBride WJ (1997a) GABA_A receptor blockade in the anterior ventral tegmental area increases extracellular levels of dopamine in the nucleus accumbens of rats. *J Neurochem* **69:**137–143.

Ikemoto S, Murphy JM, and McBride WJ (1997b) Self-infusion of GABA_A antagonists directly into the ventral tegmental area and adjacent regions. *Behav Neurosci* **111:**369–380.

Institute of Laboratory Animal Resources (1996) *Guide for the Care and Use of Laboratory Animals* 7th ed. Institute of Laboratory Animal Resources, Commission on Life Sciences, National Research Council, Washington, DC.

Jhou TC, Fields HL, Baxter MG, Saper CB, and Holland PC (2009) The rostromedial tegmental nucleus (RMTg), a GABAergic afferent to midbrain dopamine neurons, encodes aversive stimuli and inhibits motor responses. *Neuron* **61:**786–800.

Johnson SW and North RA (1992a) Opioids excite dopamine neurons by hyperpolarization of local interneurons. *J Neurosci* **12:**483–488.

Johnson SW and North RA (1992b) Two types of neurone in the rat ventral tegmental area and their synaptic inputs. *J Physiol* **450:**455–468.

Kalivas PW (1993) Neurotransmitter regulation of dopamine neurons in the ventral tegmental area. *Brain Res Brain Res Rev* **18:**75–113.

Lammel S, Hetzel A, Häckel O, Jones I, Liss B, and Roeper J (2008) Unique properties of mesoprefrontal neurons within a dual mesocorticolimbic dopamine system. *Neuron* **57:**760–773.

Majchrowicz E and Hunt WA (1976) Temporal relationship of the induction of tolerance and physical dependence after continuous intoxication with maximum tolerable doses of ethanol in rats. *Psychopharmacology (Berl)* **50:**107–112.

Mansour A, Fox CA, Akil H, and Watson SJ (1995) Opioid-receptor mRNA expression in the rat CNS: anatomical and functional implications. *Trends Neurosci* **18:**22–29.

Mansour A, Fox CA, Thompson RC, Akil H, and Watson SJ (1994) μ-Opioid receptor mRNA expression in the rat CNS: comparison to μ-receptor binding. *Brain Res* **643:**245–265.

Margolis EB, Hjelmstad GO, Bonci A, and Fields HL (2003) κ-Opioid agonists directly inhibit midbrain dopaminergic neurons. *J Neurosci* **23:**9981–9986.

Margolis EB, Lock H, Chefer VI, Shippenberg TS, Hjelmstad GO, and Fields HL (2006a) κ Opioids selectively control dopaminergic neurons projecting to the prefrontal cortex. *Proc Natl Acad Sci U S A* **103:**2938–2942.

Margolis EB, Lock H, Hjelmstad GO, and Fields HL (2006b) The ventral tegmental area revisited: is there an electrophysiological marker for dopaminergic neurons? *J Physiol* **577:**907–924.

Okamoto T, Harnett MT, and Morikawa H (2006) Hyperpolarization-activated cation current (Ih) is an ethanol target in midbrain dopamine neurons of mice. *J Neurophysiol* **95:**619–626.

Paxinos G and Watson C (2007) *The Rat Brain in Stereotaxic Coordinate*s, 6th edition, Academic Press, New York.

Pidoplichko VI, DeBiasi M, Williams JT, and Dani JA (1997) Nicotine activates and desensitizes midbrain dopamine neurons. *Nature* **390:**401–404.

Rodd ZA, Bell RL, Kuc KA, Zhang Y, Murphy JM, and McBride WJ (2005a) Intracranial self-administration of cocaine within the posterior ventral tegmental area of Wistar rats: evidence for involvement of serotonin-3 receptors and dopamine neurons. *J Pharmacol Exp Ther* **313:**134–145.

Rodd ZA, Bell RL, Zhang Y, Murphy JM, Goldstein A, Zaffaroni A, Li TK, and McBride WJ (2005b) Regional heterogeneity for the intracranial self-administration of ethanol and acetaldehyde within the ventral tegmental area of alcohol-preferring (P) rats: involvement of dopamine and serotonin. *Neuropsychopharmacology* **30:**330–338.

Rodd ZA, Oster SM, Ding ZM, Toalston JE, Deehan G, Bell RL, Li TK, and McBride WJ (2008) The reinforcing properties of salsolinol in the ventral tegmental area: evidence for regional heterogeneity and the involvement of serotonin and dopamine. *Alcohol Clin Exp Res* **32:**230–239.

Rodd-Henricks ZA, McKinzie DL, Crile RS, Murphy JM, and McBride WJ (2000) Regional heterogeneity for the intracranial self-administration of ethanol within the ventral tegmental area of female Wistar rats. *Psychopharmacology (Berl)* **149:**217–224.

Sara Y, Bal M, Adachi M, Monteggia LM, and Kavalali ET (2011) Use-dependent AMPA receptor block reveals segregation of spontaneous and evoked glutamatergic neurotransmission. *J Neurosci* **31:**5378–5382.

Sarti F, Borgland SL, Kharazia VN, and Bonci A (2007) Acute cocaine exposure alters spine density and long-term potentiation in the ventral tegmental area. *Eur J Neurosci* **26:**749–756.

Stobbs SH, Ohran AJ, Lassen MB, Allison DW, Brown JE, and Steffensen SC (2004) Ethanol suppression of ventral tegmental area GABA neuron electrical transmission involves *N*-methyl-D-aspartate receptors. *J Pharmacol Exp Ther* **311:**282–289.

Tan KR, Brown M, Labouèbe G, Yvon C, Creton C, Fritschy JM, Rudolph U, and Lüscher C (2010) Neural bases for addictive properties of benzodiazepines. *Nature* **463:**769–774.

Theile JW, Morikawa H, Gonzales RA, and Morrisett RA (2008) Ethanol enhances GABAergic transmission onto dopamine neurons in the ventral tegmental area of the rat. *Alcohol Clin Exp Res* **32:**1040–1048.

Theile JW, Morikawa H, Gonzales RA, and Morrisett RA (2009) Role of 5-hydroxytryptamine 2C receptors in Ca^{2+}-dependent ethanol potentiation of GABA release onto ventral tegmental area dopamine neurons. *J Pharmacol Exp Ther* **329:**625–633.

Thomas MJ, Malenka RC, and Bonci A (2000) Modulation of long-term depression by dopamine in the mesolimbic system. *J Neurosci* **20:**5581–5586.

Waddington JL and Cross AJ (1978) Neurochemical changes following kainic acid lesions of the nucleus accumbens: implications for a GABAergic accumbal-ventral tegmental pathway. *Life Sci* **22:**1011–1014.

Walaas I and Fonnum F (1980) Biochemical evidence for γ-aminobutyrate containing fibres from the nucleus accumbens to the substantia nigra and ventral tegmental area in the rat. *Neuroscience* **5:**63–72.

Wooltorton JR, Pidoplichko VI, Broide RS, and Dani JA (2003) Differential desensitization and distribution of nicotinic acetylcholine receptor subtypes in midbrain dopamine areas. *J Neurosci* **23:**3176–3185.

Xiao C, Shao XM, Olive MF, Griffin WC 3rd, Li KY, Krnjević K, Zhou C, and Ye JH (2009) Ethanol facilitates glutamatergic transmission to dopamine neurons in the ventral tegmental area. *Neuropsychopharmacology* **34:**307–318.

Xiao C and Ye JH (2008) Ethanol dually modulates GABAergic synaptic transmission onto dopaminergic neurons in ventral tegmental area: role of μ-opioid receptors. *Neuroscience* **153:**240–248.

Xiao C, Zhang J, Krnjević K, and Ye JH (2007) Effects of ethanol on midbrain neurons: role of opioid receptors. *Alcohol Clin Exp Res* **31:**1106–1113.

Ye JH, Zhang J, Xiao C, and Kong JQ (2006) Patch-clamp studies in the CNS illustrate a simple new method for obtaining viable neurons in rat brain slices: glycerol replacement of NaCl protects CNS neurons. *J Neurosci Methods* **158:**251–259.

Yim CY and Mogenson GJ (1980) Electrophysiological studies of neurons in the ventral tegmental area of Tsai. *Brain Res* **181:**301–313.

Zhang TA, Placzek AN, and Dani JA (2010) In vitro identification and electrophysiological characterization of dopamine neurons in the ventral tegmental area. *Neuropharmacology* **59:**431–436.

Address correspondence to: Jiang-Hong Ye, Department of Anesthesiology, UMDNJ, New Jersey Medical School, 185 South Orange Avenue, Newark, NJ 07103. E-mail: ye@umdnj.edu